JOURNAL OF VIROLOGY, July 1993, p. 3901–3907
0022-538X/93/073901-07$02.00/0

Vol. 67, No. 7

# Assembly of Theiler's Virus Recombinants Used in Mapping Determinants of Neurovirulence

A. E. PRITCHARD, K. JENSEN, AND H. L. LIPTON*

*Department of Neurology, University of Colorado Health Sciences Center, Denver, Colorado 80262*

Received 23 December 1992/Accepted 31 March 1993

**A major determinant of neurovirulence for the GDVII strain of Theiler's virus, a murine picornavirus, was mapped to the P1 capsid protein region. Chimeric viruses were constructed by using sequences from the 5′ noncoding and P1 regions of the virulent GDVII strain to replace equivalent regions of the less virulent BeAn strain. Neurovirulence in mice progressively increased as larger regions of BeAn capsid protein-encoding sequences were replaced. The in vitro growth characteristics of the chimeras showed that some chimeras were growth delayed in BHK-21 cells even though the viral constructs exhibited larger plaque sizes, were less temperature sensitive, and were more thermally stable than BeAn. Examination of assembly intermediates revealed an altered pentamer conformation and delayed empty capsid formation for the growth-compromised viruses. For these constructs, their chimeric nature inadvertently resulted in virion assembly defects that complicated finer-scale mapping of the determinants of virulence within the capsid region. These results demonstrate the importance of determining in vitro growth characteristics of chimeras to correctly decipher the significance of their phenotypes. VP1 does not contain a complete determinate for virulence because a chimera with VP1-encoding sequences from GDVII in an otherwise BeAn virus has an attenuated phenotype but is not growth compromised in vitro. The source of sequences, BeAn or GDVII, in the 5′ noncoding region had only slight effects on the virulence of recombinant constructs.**

Theiler's murine encephalomyelitis virus (TMEV) infection in mice is a valuable model for understanding the molecular biology of viral neurovirulence, persistence, and virus-induced demyelination. Members of this picornavirus genus can be divided into two groups based on neurovirulence characteristics after intracerebral inoculation of mice: (i) the highly virulent viruses, represented by the GDVII strain, which produce fatal encephalitis in mice, and (ii) the less virulent strains such as BeAn and DA, which are capable of producing a persistent infection that is associated with chronic, inflammatory demyelinating disease (8).

Numerous papers have been published in recent years on attempts to map in the TMEV genome the determinants for virulence, persistence, and demyelination (1–3, 10, 13, 14, 16, 17). Much attention has been focused on the P1 region, in particular VP1 (13, 17), but the 5′ noncoding region (5′NCR) has also been studied extensively (10, 14, 16), and one report emphasizes the apparent multigenic nature of the determinants for virulence (16). The three classes of determinants probably do not map to the same location, but these characteristics are related and may be tightly linked. Persistence and chronic demyelination are closely associated, while virulent strains have never been shown to persist even when inoculated at low doses (9). On the other hand, there are examples of less virulent constructs that do not persist (10).

In this communication, we concentrate on the mapping of virulence in the leader and P1 regions. The less virulent BeAn and DA strains are characterized by a $10^6$-fold reduction in 50% mean lethal dose ($LD_{50}$) in comparison with the virulent GDVII strain. Most mapping studies to date utilize the construction of interstrain chimeras. Results of these experiments suggest that the P1 region contains a major determinant of virulence (1, 2, 13, 17). Chimeras with GDVII sequences between the downstream end of the 5′NCR and the 2A gene, in an otherwise BeAn (or DA) virus, are significantly more virulent than the attenuated strain (1, 13). The roles of the P2 region and individual genes of the P1 region need further clarification.

Our approach to finer-scale mapping was to attempt the construction of a virulent chimera by progressively replacing BeAn sequences with GDVII sequences starting with the VP1 capsid protein gene at the 3′ end of the P1 region. To understand the molecular basis for the phenotypes of the resulting chimeras, it was necessary to characterize their in vitro growth properties. Previous studies have noted a close correspondence between virulence, large plaque size, and temperature insensitivity. We were interested in determining the mechanism for the relative attenuation of BeAn to aid our understanding of its ability to persist and demyelinate. However, it is obvious there are many ways to attenuate a virus that are irrelevant to the mechanism of attenuation of BeAn (14). We demonstrate here that the P1 region does contain a major determinant of virulence. But we also show the limitations of the chimeric approach to mapping these determinants, since some constructs exhibited compromised in vitro growth characteristics. It is important to consider the possibility of this inadvertent consequence when interpreting the results of mapping experiments.

## MATERIALS AND METHODS

**Construction of chimeras.** Recombinant virus cDNA clones in pGEM-3 vectors were constructed by using full-length BeAn and GDVII cDNA clones previously described (1, 10). GDVII sequences were inserted into BeAn cDNA by using a unique *Xho*I site at the VP1/2A junction. An *Xho*I site, absent in wild-type GDVII, was introduced by a T-to-C mutation, using site-directed mutagenesis (6). The region containing the *Xho*I site in the resulting clone was verified by sequencing.

DNA from clones was linearized and transcribed, and

* Corresponding author.

BHK-21 cells were transfected as described previously (14). Progeny virus stocks were prepared after an additional passage in BHK-21 cells. Recombinant constructs were verified by preparing polymerase chain reaction-amplified cDNA fragments derived from chimeric viruses (14). Important regions of the polymerase chain reaction-amplified DNA, such as chimeric boundary areas, were confirmed by sequencing or by digestion with appropriate restriction enzymes.

**Cell culture.** BHK-21 cells were grown in 60-mm-diameter plates in Dulbecco's modified Eagle medium supplemented with 2 mM L-glutamine, 10% tryptose phosphate broth (GIBCO), and 5% iron-supplemented bovine calf serum (HyClone). Plaque size, virus growth, and temperature sensitivity of the chimeras were determined by standard plaque assay on BHK-21 cell monolayers as described previously (9). Infected cells were incubated for 3 days at 37°C, and plaques were identified by staining with 0.1% crystal violet.

**One-step growth curves.** BHK-21 cell monolayers on 35-mm-diameter plates were infected with virus at a multiplicity of infection of 10. After a 30-min adsorption period at 37°C, inocula were removed, cells were washed once with serum-free medium, and incubation was continued in complete medium. At indicated times, cells and supernatants were harvested together and sonicated to release virus. Plaque assays performed at 37°C quantitated the PFU per cell present at each time point. Titers from plaque assays were performed in duplicate or triplicate and averaged for the data shown.

**Labeling of viral proteins.** BHK-21 cell monolayers were infected with virus as described above. One hour prior to addition of label, medium was removed and cells, after rinsing, were covered with methionine-free or leucine-free minimal essential medium containing 10 mM sodium pyruvate and 1% glutamine and incubated for 1 h. Medium was then replaced by that containing 100 μCi of L-[$^{35}$S]methionine (1,000 Ci/mmol; NEN) or L-[4,5-$^{3}$H]leucine (133 Ci/mmol; Amersham). Following incubation for the indicated times, cells were harvested after removal of medium and two rinses with phosphate-buffered saline. Cell lysates were prepared in 0.4 ml of lysis buffer (1% Triton X-100, 1% sodium deoxycholate, 150 mM NaCl, 1 mM EDTA, 50 mM Tris [pH 7.4]) and centrifuged at 4°C in an Eppendorf Microfuge for 10 min. Supernatants were then either layered on sucrose gradients or immunoprecipitated directly.

**Sucrose gradients.** Cell lysates were fractionated on 11-ml 5 to 20% or 15 to 30% sucrose gradients prepared in lysis buffer. Gradients were centrifuged in an SW41 (Beckman) rotor at 35,000 rpm for 16 h (5 to 20%) or at 18,000 rpm for 12 h (15 to 30%). Fractions (0.5 ml) were collected by pumping from the bottom of the gradient and then immunoprecipitated. When fractions containing both L-[$^{35}$S]methionine L-[4,5-$^{3}$H]leucine were counted in a scintillation counter, the windows were appropriately adjusted to minimize overlap.

**Immunoprecipitation.** Fractions of sucrose gradients or unfractionated cell lysates were incubated with shaking overnight at 4°C with 5 μl of rabbit polyclonal anti-BeAn serum. Samples were then incubated with 40 μl of a suspension of formalin-fixed *Staphylococcus aureus* cells (Immunoprecipitin; GIBCO-BRL) at 4°C for 2 h with shaking. After centrifugation for 5 min, pellets were resuspended in lysis buffer and the washes were repeated twice. Final pellets were suspended in 30 μl of reducing sample buffer (1.4 M 2-mercaptoethanol, 4.6% sodium dodecyl sulfate [SDS], 125 mM Tris [pH 6.8], 20% glycerol) and boiled for 3 min. Aliquots were quantitated for radioactivity in a scintillation counter or analyzed by SDS–12% polyacrylamide gel electrophoresis (PAGE) (7) followed by autoradiography.

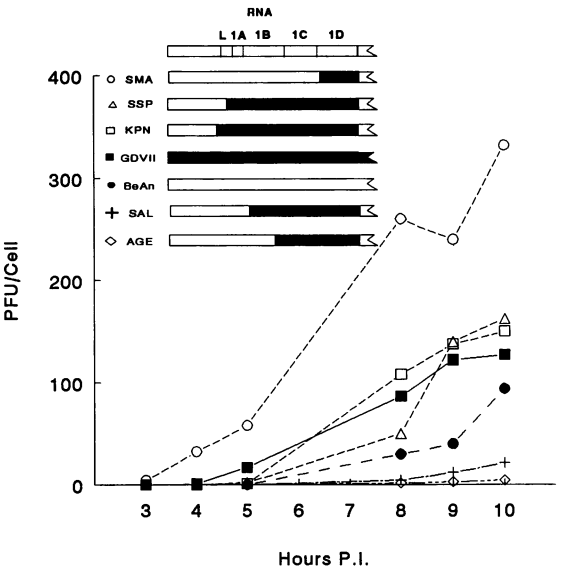


FIG. 1. One-step growth titers as a function of hours after infection of BHK-21 cells with parental and chimeric virus strains. For each growth curve, the GDVII and BeAn composition of the chimera's P1 region is depicted.

**Thermal stability.** Virus, at different dilutions in Dulbecco's modified Eagle medium, was incubated at 45°C. At various times, 800-μl aliquots were removed and titers were determined by plaque assay on BHK-21 cell monolayers at 37°C.

**Animal inoculations and determination of $LD_{50}$.** The $LD_{50}$ values were determined by using 6- to 10-week-old CD-1 mice inoculated in the right cerebral hemisphere with 10-fold dilutions (five to six mice per dilution) of parental and mutant viruses in 30 μl as previously described (1, 10). $LD_{50}$ values of $>10^6$ could not be more precisely determined because of the limiting concentration of the viral stocks available.

## RESULTS

**Viral chimeras of BeAn and GDVII.** Since previous studies have suggested that the major determinant of virulence for the GDVII strain is located in the capsid P1 region (1, 2, 13, 17), we constructed a series of chimeras in which GDVII sequences progressively replaced the BeAn genome starting at the 3′ end of the capsid protein genes. We started with VP1 replacements because of previous indications that this protein plays an important role in virulence and demyelination (4, 11, 13, 17, 18). We hoped that a virulent chimera would be obtained when the minimal GDVII determinants of virulence were included. Some of the chimeras that were constructed are shown in Fig. 1. All chimeras have a common boundary of GDVII sequences ending at an *Xho*I site located at the 3′ end of the VP1 gene. The 5′ end of the inserted GDVII sequences are at various restriction sites, whose names were used for viral nomenclature. In general, each of the five chimeras progressively includes one additional gene of inserted GDVII sequences. For example, the SMA chimera contains GDVII sequences in the VP1-encod-

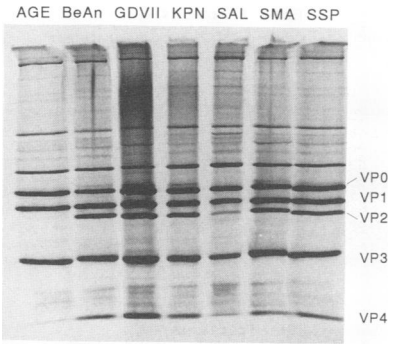


FIG. 2. Autoradiogram showing viral protein expression of chimeric constructs. BHK-21 cells were infected with virus and labeled with L-[$^{35}$S]methionine between 1 and 7 h p.i. Protein from cell lysates was immunoprecipitated, and aliquots were analyzed by SDS-PAGE.

ing region, while the AGE chimera has GDVII in VP3 and VP1.

To characterize the resulting chimeras, one-step growth curves were obtained (Fig. 1). The virulent GDVII strain grew slightly faster than the less virulent BeAn strain in BHK-21 cells. Most of the viral chimeras grew as well as or better than (the SMA chimera; Fig. 1) the parental strains except two: the AGE and SAL chimeras. These viruses have GDVII sequences in VP3 plus VP1 and in VP2 plus VP3 plus VP1, respectively (the recombinant boundaries, however, are not coincident with the coat protein boundaries). In the first 10 h postinfection (p.i.), these two chimeras were significantly retarded in growth compared with the other viral strains shown. However, after 24 h, the virus titers were comparable for all of the strains (not shown). The AGE and SAL strains were growth delayed.

The kinetic block in the growth of these chimeras conceivably could be anywhere in the viral cycle, including receptor attachment, cell entry, uncoating, replication, translation, or assembly. The amounts of viral products produced late in the cycle for the various strains were determined to temporally locate the block. BHK-21 cells were infected with virus and continuously labeled with L-[$^{35}$S]methionine between 1 and 7 h p.i. Total cytoplasmic proteins were harvested, and viral proteins were immunoprecipitated and analyzed by SDS-PAGE (Fig. 2). Viral capsid protein bands were identified by their molecular weights. As shown in Fig. 2, all of the chimeric and parental strains exhibited similar amounts of VP0, VP1, and VP3. The growth-compromised chimeras, AGE and SAL, apparently were not grossly blocked at steps prior to translation and polyprotein processing. However, for these two chimeras, the amounts of VP2 and VP4 were significantly less than in the other strains at this time point (Fig. 2). AGE showed neither of these capsid proteins, while SAL had discernible but reduced VP2 and VP4 bands compared with the noncompromised strains. Since VP2 and VP4 are cleaved from VP0 as a final step in virion assembly, it appears the AGE and SAL chimeras are blocked late in the viral cycle.

It is not obvious why the compromised chimeras did not accumulate more VP0 relative to the other strains. There is experimental evidence, obtained with poliovirus strains defective in assembly, that capsid proteins in lower-order structures such as protomers or pentamers are degraded at a greater rate than are proteins in empty capsids and virions (12). The AGE and SAL chimeras are defective in assembly of empty capsids and virions (see below), and it is possible that the VP0-containing pentamers are degraded and VP0 does not accumulate.

**Virion assembly.** To verify these apparent defects, intermediates in virion assembly were identified by sucrose gradient centrifugation. BHK-21 cells were infected with virus, and proteins were labeled with L-[$^{35}$S]methionine between 5.5 and 6.25 h p.i. Total cytoplasmic proteins were harvested and fractionated on 5 to 20% sucrose gradients. Following immunoprecipitation with polyclonal BeAn antisera, radioactivity in the fractions was assayed, and aliquots of representative fractions were analyzed by SDS-PAGE. Gradient profiles for BeAn and AGE are shown in Fig. 3. The protomer (fractions 16 to 20) and pentamer (fractions 5 to 12) peaks were identified by their protein composition (Fig. 3) and comparison with previous picornavirus sucrose gradients (15). The growth-compromised AGE virus exhibited a pentamer peak that was smaller and shifted in position relative to that of the BeAn virus.

To confirm the apparent relative shift in the pentamer peaks, BHK-21 cells were infected with virus, the parental BeAn viral proteins were labeled with L-[4,5-$^{3}$H]leucine, and the viral proteins of other strains were labeled with L-[$^{35}$S]methionine. This permitted assembly intermediates from two viral strains, a BeAn parental reference and a chimera, to be fractionated and identified on the same 5 to 20% gradient. In Fig. 4, the gradients comparing the parental BeAn and GDVII strains with each other and BeAn with the SMA chimera showed no shifts in peak positions. In contrast, the gradients comparing the BeAn strain with either of the growth-compromised AGE and SAL chimeric viruses showed that the pentamer peaks of these chimeras were shifted, compared with the BeAn pentamer, toward the bottom of the gradient. This result probably indicates an altered conformation for these chimeric pentamers, since the composition of the peaks for the parental and recombinant viruses appeared identical (Fig. 3).

There was some variation in the relative heights of pentamer and protomer peaks for each strain shown in Fig. 4, but the significance of this observation is not clear. The BeAn, GDVII, and AGE pentamer peaks were higher than their corresponding protomer peaks, while the converse was true for SMA and SAL chimera peaks. Since the SMA chimera grew extremely well in BHK-21 cells, and the SAL chimera was less growth compromised than the AGE chimera (Fig. 1), there is no obvious correlation between relative peak heights and growth characteristics.

To investigate assembly of empty capsids and virions, BHK-21 cells were infected with BeAn or AGE virus, proteins were labeled with L-[$^{35}$S]methionine, and cytoplasmic extracts were fractionated on 15 to 30% sucrose gradients. Figure 5 shows very little empty capsid or mature virion for the growth-compromised chimeras SAL and AGE, compared with the parental strains, up to 6.5 h p.i. On the basis of the growth curves (Fig. 1), little mature virion for the AGE or SAL viruses was expected. When infected cells were labeled from 1 to 6 h p.i., more GDVII than BeAn virions were detected on the gradients, but no significant amounts of SAL virions or empty capsids were measured (Fig. 5). The identity of the parental virion peak was determined by the composition of proteins in the peaks (Fig. 6) and comparison with the sedimentation of purified BeAn virions containing [$^{32}$P]RNA (Fig. 5). The protein gel of the fractions (Fig. 6) showed that VP2 and VP4 were produced as the final step in virion maturation of BeAn.

The sucrose gradients of the virion assembly intermedi-

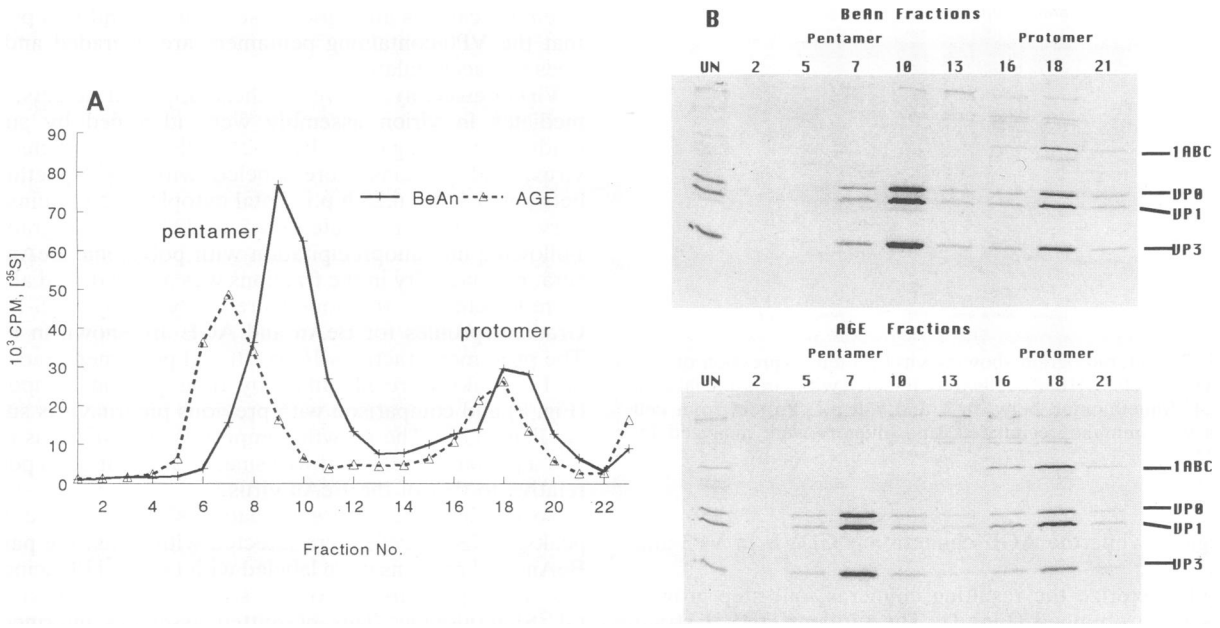


FIG. 3. Five to 20% sucrose gradients of capsid structures. BHK-21 cells were infected with virus, and proteins were labeled with L-[$^{35}$S]methionine between 5.5 and 6.25 h p.i. Lysates of BeAn and AGE infected cells were sedimented through separate gradients; fractions were collected and immunoprecipitated. Aliquots of 15 μl were scintillation counted (A; bottom of gradient is on the left), and 8 μl of selected fractions was analyzed by SDS-PAGE (B). Also shown are gel lanes for unfractionated immunoprecipitated lysates (UN).

ates showed that the growth-delayed chimeras AGE and SAL were normal in protein production and processing up to the formation of protomers. However, these chimeras had abnormal pentamer assembly, as evidenced by shifted peaks in gradients (Fig. 4). They also exhibited considerable delay in the formation of empty capsids and mature virions (Fig. 5 and 6). The defect in the growth cycle for these compromised strains is therefore in the assembly of pentamers and empty capsids.

**Virulence.** The virulence of the virus strains shown in Fig. 1 were determined in CD-1 mice and are expressed as $LD_{50}$ in Table 1. Some of the strains discussed above were further modified by replacing most of the BeAn 5′NCR sequences with the corresponding GDVII nucleotides, and these additional chimeric strains are also listed in Table 1. The data show that GDVII sequences extending from the *Age*I site near the 3′ end of sequences encoding VP2, from the *Sma*I site near the VP3/VP1 boundary, or from the *Mlu*I site near the middle of sequences encoding VP1 to the end of the P1 region did not result in a more virulent virus. As GDVII sequences were progressively added 5′ to the *Age*I site, virulence increased so that the KPN chimera, with GDVII sequences in all of the leader and P1 regions, was nearly as virulent as the GDVII parent. These results show that most of the GDVII determinants of virulence map to the P1 region. Further localization within the capsid region is precluded in these experiments because of the assembly defects that were inadvertently introduced. The source of the 5′NCR sequences, BeAn or GDVII, had only a slight effect on the virulence. Chimera 2C, with BeAn sequences only in the 5′NCR and first portion of the leader gene in an otherwise GDVII virus, was found to be virulent ($LD_{50}$ of $10^{1.9}$).

Plaque sizes of the various chimeras (Table 1) correlated with virulence. As more of the P1 region was replaced with GDVII sequences, plaque sizes increased. All virulent strains had large plaques, but it has been previously noted that some large-plaque phenotypes are not virulent (1, 14). Temperature sensitivity, expressed as efficiency of plaquing at 39.8°C compared with 33°C, also correlated with GDVII sequences in the P1 region (Table 1). In this case, inefficient plaque formation at 39.8°C appeared to map more narrowly to just VP1. Both temperature sensitivity and plaque size appeared to be necessary but not sufficient characteristics for virulence.

Thermal stabilities of several chimeras were also determined (not shown). The decrease in viral stock titers was measured as a function of incubation time at 45°C before plaquing at 37°C. BeAn was dramatically less stable than all of the other strains; there was a 99% decrease in titer after a 10-min incubation at 45°C. The other strains exhibited a 40 to 85% decrease after 1 h. Replacement of just the BeAn VP1 sequences with corresponding GDVII sequences (SMA chimera) significantly increased the stability. Among the chimeras, there was no correlation between the relative amount of GDVII sequences in the P1 region and thermal stability. These results show that defects in the growth-compromised strains are not due to thermal instability.

## DISCUSSION

The viral chimeras characterized in this study demonstrate that most of the GDVII determinants of virulence reside in the P1 region. When the BeAn sequences encoding VP1, VP2, and VP3 are replaced by corresponding GDVII sequences (SAL chimera), more than 90% of the virulence is restored. SAL has a $LD_{50}$ of 79,000, which is less than 10% of the difference between the $LD_{50}$ values of $>10^6$ for BeAn and 10 for GDVII. Similarly, an $LD_{50}$ of 3,200 for SSP corresponds to a 99% restoration of the virulence. Since we have also shown that the SAL chimera is growth delayed in

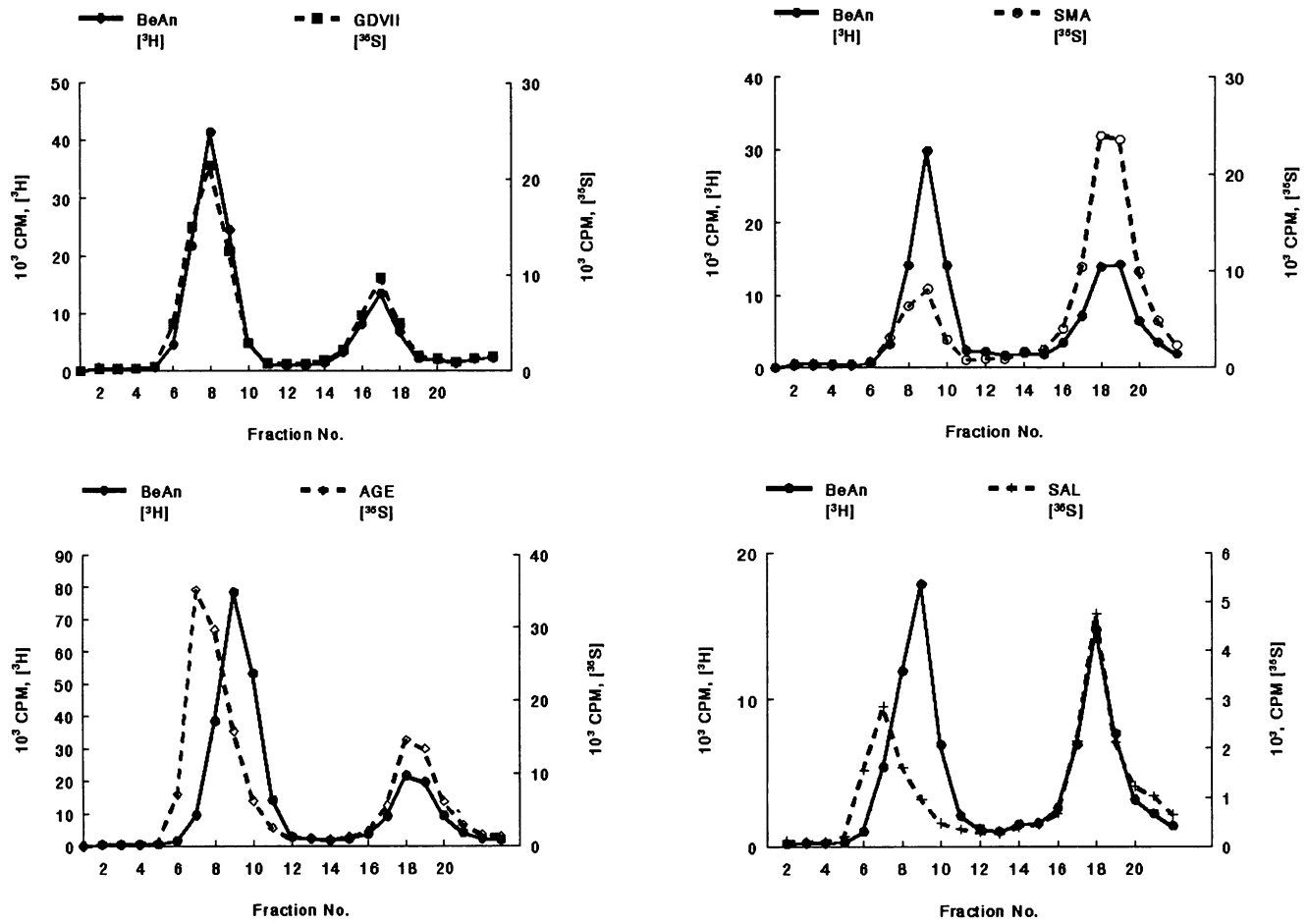


FIG. 4. Five to 20% sucrose gradients of capsid structures. BHK-21 cells were infected with virus, and proteins were labeled with L-[$^{35}$S]methionine or L-[4,5-$^{3}$H]leucine (BeAn-infected cells) between 5 and 5.75 h p.i. (except for the BeAn-with-AGE experiment, in which labeling was between 5.5 and 6.25 h p.i.). For each experiment, the L-[4,5-$^{3}$H] lysate of BeAn-infected cells was mixed with the L-[$^{35}$S] lysate of chimera- or GDVII-infected cells, and the mixture then was sedimented through gradients. Fractions were collected and immunoprecipitated. Aliquots of 10 μl were scintillation counted.

vitro, its $LD_{50}$ represents an upper limit in terms of mapping the GDVII virulence (see below).

This virulence mapping is a continuation of previous attempts. The results of Calenoff et al. (1), McAllister et al. (13), Fu et al. (3), and Stein et al. (16) were obtained by using chimeras with one of the recombinant boundaries usually outside the coat protein region. The results presented in this communication, which are more narrowly concentrated on the P1 region, are not inconsistent with these previous results.

However, these previous studies on virulence, as well as those on the related persistence phenotype (2, 17), did not include measurements of the in vitro growth characteristics of the recombinant viruses. Such experiments are critical since we have shown that at least some of the chimeras inadvertently possessed assembly defects that additionally affected neurovirulence and therefore masked measuring the specific determinants that we were seeking. Chimeras AGE (one GDVII-encoded amino acid at the end of VP2 plus all amino acids in VP3 and VP1) and SAL (GDVII-encoded amino acids in VP2, VP3, and VP1) were growth delayed in vitro compared with the parental strains (Fig. 1). These chimeras were delayed in empty capsid and mature virion formation (Fig. 5). On sucrose gradients, their pentamer subunits were shifted in position relative to all other strains studied (Fig. 4). Their $LD_{50}$s therefore cannot be regarded as valid for use in mapping GDVII determinants for neurovirulence. Although these chimeras were compromised in assembly, their mature virions were thermally stable.

The assembly defects are presumably due to incongruent interactions between coat proteins from BeAn and GDVII in the chimeric pentamer subunit. The only mixed interaction unique to the compromised AGE and SAL chimeras is between a GDVII VP3 and a BeAn VP4 (within VP0 of the pentamer). Improper alignments between these proteins may deform the shape of the pentamer and inhibit formation of empty capsids. Deformation of the pentamer may also affect the subsequent cleavage of VP0 to VP2 plus VP4, thereby destabilizing formation of the mature virion from the empty capsid, but no conclusion in this regard can be made from the data presented here. A comparison between GDVII and BeAn amino acid sequences in the entire capsid region shows a difference of 4.8%. Of the individual capsid proteins, VP1 amino acids have the greatest difference (6.9%) and VP3 residues have the least difference (3.4%).

In contrast to the AGE and SAL chimeras, the SMA

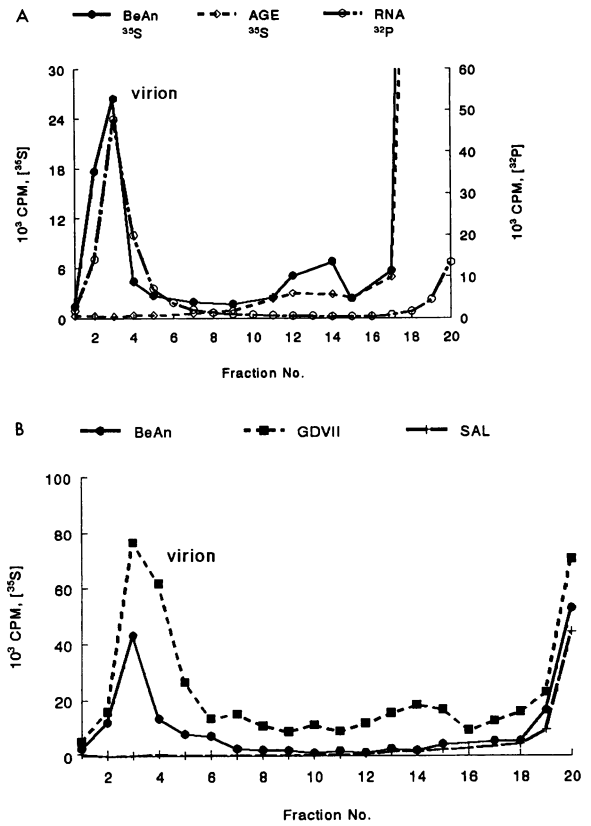


FIG. 5. Fifteen to 30% sucrose gradients of capsid structures. BHK-21 cells were infected with virus, and proteins were labeled with L-[$^{35}$S]methionine between 5.5 and 6.5 h p.i. (A) or between 1 and 6 h p.i. (B). Lysates of infected cells were sedimented through separate gradients, fractions were collected and immunoprecipitated, and aliquots were scintillation counted. In a separate gradient, purified BeAn virion containing [$^{32}$P]RNA was sedimented, fractions were collected, and Cerenkov radiation of aliquots was quantitated (A). The bottom of the gradient is on the left.

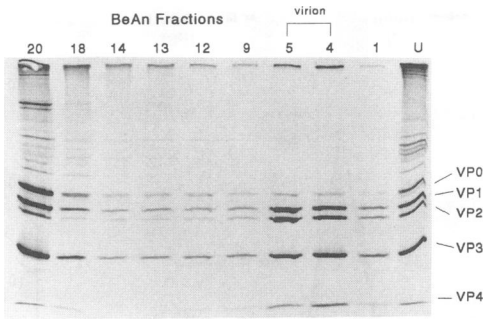


FIG. 6. SDS-PAGE analysis of 15 to 30% sucrose gradient fractions. Selected aliquots from fractions of the BeAn gradient shown in Fig. 5 were electrophoresed along with an unfractionated sample (U). Fractions from the bottom of the gradient are on the right.

chimera exhibits no compromised growth characteristics in vitro. In this construct, with the exception of the second amino acid, the VP1 sequence is GDVII. It grows well in tissue culture (Fig. 1), is thermally stable, has a larger plaque size, and is less temperature sensitive than BeAn (Table 1). In fact, it grows better than the virulent GDVII strain in BHK-21 cells (Fig. 1). However, in vivo, this chimera replicates more like a less virulent strain. Brains of five mice, sacrificed 5 days after inoculation with $10^6$ PFU of the SMA chimera, were found to have an average virus titer of $6.7 \times 10^3$ PFU/g. This value can be compared with titers of $10^7$ PFU/g for GDVII and $10^5$ PFU/g for BeAn measured 5 days after inoculation (5).

Since we cannot detect growth defects for the SMA chimera in vitro, it is possible that its attenuated phenotype accurately reflects the absence of a complete GDVII determinant for virulence in VP1. Virulence may be possible only if the entire P1 region is GDVII as the data here suggest, but the evidence so far is inconclusive. There is little evidence to date that there is any determinant of virulence in VP1. GDVII sequences, with nucleotide substitutions from the less virulent strain DA in VP1 only, have been reported to yield an attenuated virus (pTMR9 [13]). However, recently it was determined that the phenotype described for virus R9 was due to a contamination with DA virus and that plasmid pTMR9 is not infectious (see authors' corrections for references 13 and 17). To our knowledge, there are no other published reports of chimeras with BeAn or DA substitutions in just one of the coat proteins.

Virulent chimeras with limited BeAn substitutions in an otherwise GDVII virus are easier to interpret. Chimera 2C, with BeAn sequences only from nucleotides 1 to 1142 (leader-encoding sequences start at nucleotide 1065), is nearly as virulent as GDVII (Table 1). This result extends our previous report that BeAn sequences up to nucleotide 933 in the 5'NCR are not attenuating (chimera 5C [14]). The SSP chimera, identical to chimera 2C in the 5' half of the virus, has BeAn sequences also 3' to the P1 region. Its virulence is reduced by a factor of $10^{1.6}$ relative to that of chimera 2C. Either there are some determinants of virulence 3' to the P1 region or improper interactions between proteins from the BeAn and GDVII regions affect neurovirulence.

In conclusion, we have shown that the capsid region of TMEV contains determinants of virulence, temperature sensitivity, thermal stability, and plaque size. These phenotypes appear to be linked. In finer-scale mapping experiments, growth characteristics of chimeras must be carefully consid-

TABLE 1. Properties of P1 region recombinants

| Virus | Genomic structure | Log $_{10}$ $LD_{50}$ | Plaque Size(mm) | EOP[a] |
|---|---|---|---|---|
| | Kb 0 1 VP4 2 3 4 5 | | | |
| BeAn | L VP2 VP3 VP1 | >6 | 1 | <$10^{-6}$ |
| GDVII | | <1 | 3-5 | 0.46 |
| 5' MLU | 1142 3510 3825 | >6 | <1 | 0.002 |
| 5' SMA | 1142 3095 | >6 | 1-2 | 0.046 |
| SMA | 3095 | >6 | <1 | 0.43 |
| 5' AGE | 1142 2214 | >6 | 1-2 | 0.53 |
| AGE | 2214 | >6 | 1.5-2.5 | ND |
| SAL | 1597 | 4.9 | 3-4 | 1.2 |
| SSP | 1142 | 3.5 | 3-5 | 0.61 |
| KPN | 933 | 2.5 | 3-5 | 0.48 |
| Chi 2C | 1142 | 1.9 | 3-5 | ND |

[a] Efficiency of plaquing (EOP) is the ratio of the titer at 39°C to that at 33°C. ND, not determined.

ered to avoid inadvertent defects. We are currently replacing small regions of the GDVII virus with corresponding BeAn sequences. If the phenotype is virulent, the particular BeAn sequence can be ruled out as a determinant of virulence or attenuation.

## ACKNOWLEDGMENTS

We acknowledge critical readings of the manuscript by Pradip Bandyopadhyay and Todd Knauf.

This research was supported by National Multiple Sclerosis Society grant RG 1815-A-6, Public Health Service grant NS21913 from the National Institutes of Health, and funds from the Leiper Foundation.

## REFERENCES

1. **Calenoff, M. A., K. S. Faaberg, and H. L. Lipton.** 1990. Genomic regions of neurovirulence and attenuation in Theiler's murine encephalomyelitis virus. Proc. Natl. Acad. Sci. USA **87:**978–982.
2. **Fu, J., M. Rodriguez, and R. Roos.** 1990. Strains from both Theiler's virus subgroups encode a determinant for demyelination. J. Virol. **64:**6345–6348.
3. **Fu, J., S. Stein, L. Rosenstein, T. Bodwell, M. Routbort, B. Semler, and R. Roos.** 1990. Neurovirulence determinants of genetically engineered Theiler viruses. Proc. Natl. Acad. Sci. USA **87:**4125–4129.
4. **Grant, R. A., D. J. Filman, R. S. Fujinami, J. P. Icenogle, and J. M. Hogle.** 1992. Three-dimensional structure of Theiler virus. Proc. Natl. Acad. Sci. USA **89:**2061–2065.
5. **Jensen, K., A. E. Pritchard, and H. L. Lipton.** Unpublished data.
6. **Kunkel, T. A.** 1985. Rapid and efficient site-specific mutagenesis without phenotypic selection. Proc. Natl. Acad. Sci. USA **82:**488–492.
7. **Laemmli, U. K.** 1970. Cleavage of structural proteins during the assembly of the head of bacteriophage T4. Nature (London) **227:**680–685.
8. **Lipton, H. L.** 1975. Theiler's virus infection in mice: an unusual biphasic disease process leading to demyelination. Infect. Immun. **11:**1147–1155.
9. **Lipton, H. L.** 1980. Persistent Theiler's murine encephalomyelitis virus infection in mice depends on plaque size. J. Gen. Virol. **46:**169–177.
10. **Lipton, H. L., M. Calenoff, P. Bandyopadhyay, S. D. Miller, M. C. Dal Canto, S. Gerety, and K. Jensen.** 1991. The 5′ noncoding sequences from a less virulent Theiler's virus dramatically attenuate GDVII neurovirulence. J. Virol. **65:**4370–4377.
11. **Luo, M., C. He, K. S. Toth, C. X. Zhang, and H. L. Lipton.** 1992. Three-dimensional structure of Theiler murine encephalomyelitis virus (BeAn strain). Proc. Natl. Acad. Sci. USA **89:**2409–2413.
12. **Macadam, A. J., G. Ferguson, C. Arnold, and P. D. Minor.** 1991. An assembly defect as a result of an attenuating mutation in the capsid proteins of the poliovirus type 3 vaccine strain. J. Virol. **65:**5225–5231.
13. **McAllister, A., F. Tangy, C. Aubert, and M. Brahic.** 1990. Genetic mapping of the ability of Theiler's virus to persist and demyelinate. J. Virol. **64:**4252–4257. (Author's correction, **67:** 2427, 1993.)
14. **Pritchard, A. E., M. A. Calenoff, S. Simpson, K. Jensen, and H. L. Lipton.** 1992. A single base deletion in the 5′ noncoding region of Theiler's virus attenuates neurovirulence. J. Virol. **66:**1951–1958.
15. **Rueckert, R. R.** 1986. Picornaviruses and their replication, p. 357–390. *In* B. N. Fields and D. M. Knipe (ed.), Fundamental virology. Raven Press, New York.
16. **Stein, S. B., L. Zhang, and R. P. Roos.** 1992. Influence of Theiler's murine encephalomyelitis virus 5′ untranslated region on translation and neurovirulence. J. Virol. **66:**4508–4517.
17. **Tangy, F., A. McAllister, C. Aubert, and M. Brahic.** 1991. Determinants of persistence and demyelination of the DA strain of Theiler's virus are found only in the VP1 gene. J. Virol. **65:**1616–1618. (Author's correction, **67:**2427, 1993.)
18. **Zurbriggen, A. J., J. M. Hogle, and R. S. Fujinami.** 1989. Alteration of amino acid 101 within capsid protein VP1 changes the pathogenicity of Theiler's murine encephalomyelitis virus. J. Exp. Med. **170:**2037–2049.